Electrochemical and Solid-State Letters, **13** (5) B47-B49 (2010)
1099-0062/2010/13(5)/B47/3/$28.00 © The Electrochemical Society

Highly Active Carbon Supported Core-Shell PtNi@Pt Nanoparticles for Oxygen Reduction Reaction

Wenzhen Li[a,b,*,z] **and Pradeep Haldar**[a,b]

[a]*Department of Chemical Engineering, Michigan Technological University, Houghton, Michigan 49931, USA*
[b]*College of Nanoscale Science and Engineering, State University of New York at Albany, New York 12203, USA*

A carbon supported core-shell PtNi@Pt nanoparticle catalyst was synthesized through a two-step solution-phase reduction method, and it demonstrated a 5.4 times higher specific activity to an oxygen reduction reaction than a conventional Pt/C catalyst by using a rotating disk electrode in a three-compartment electrochemical cell, which could be attributed to the modified electronic structure of the Pt surface layer.
 [DOI: 10.1149/1.3313347]

Manuscript submitted October 17, 2009; revised manuscript received November 16, 2009. Published February 25, 2010.

Molecular oxygen reduction reaction (ORR) is the primary reaction taken at the cathode of fuel cells, metal–air batteries, and many electrochemical industrial processes.[1-4] ORR is a highly irreversible four-electron transfer process with very slow reaction kinetics. Even at the most active Pt surface, the overpotential at the open-circuit state is >250 mV, and the exchange current density is only 10^{-9} A/cm^2. The output power density (P) of a fuel cell is the product of the cell potential (V) and the current (I), $P = V \times I$. Raising the cell potential from 0.65 to 0.9 V leads to a 15% improvement in thermodynamic efficiency (from 44 to 60%). Extensive theoretical and experimental works have been carried out to reduce the ORR overpotential. Alloying Pt with a transitional metal M (M = Cr, Co, Fe, Ni, Cu, etc.) is able to effectively improve the kinetics of ORR.[4-18] The mechanisms proposed to date can be generally classified as geometric effects,[5] electronic effects,[6-8] OH^- adsorption weakening effects,[9-13] surface roughening effects,[14] and H_2O_2 decomposition effect.[15] A homogeneous composition and a small particle size are critical for practical Pt–M bimetallic catalysts.[2,4,12] We have recently developed a solution-phase reduction method[19,20] to prepare a carbon supported Pt–Co alloy nanoparticle (NP) electrocatalyst, which demonstrated a 2.5 times higher mass activity (MA) than the conventional Pt/C catalyst in a proton exchange membrane fuel cell.[20] In this article, we modified this solution-phase method to prepare carbon supported PtNi-core Pt-shell (PtNi@Pt/C) NPs as electrocatalysts and tested its ORR activity in a three-compartment electrochemical cell.

Experimental

The synthesis of PtNi@Pt/C was based on a solution-phase reduction method invented by IBM researchers.[21,22] The synthesis procedures are as shown in Fig. 1. $Pt(acac)_2$ (where acac is acetylacetonate) (99 mg, 0.25 mmol) and $Ni(acac)_2$ (73 mg, 0.27 mmol), 1,2-hexadecanediol (325 mg, 1.25 mmol), and phenyl ether (20 mL) were added into a flask equipped with a N_2 in/outlet, a refluxing tube, and a thermal couple. The mixture was heated by a mantle to 100°C under a blanket of N_2 for 10 min. Oleic acid (OAc, 0.08 mL, 0.25 mmol) and oleylamine (OAm, 0.09 mL, 0.25 mmol) were added at this temperature, then the mixture was heated to 200°C for 20 min, and $LiBet_3H$ was dropped into the synthesis system. The solution was heated up to 260°C for 20 min. The heating was then stopped and the mantle heater was removed as the temperature dropped to 200°C, the black reaction mixture was subsequently cooled down to room temperature. After ethanol (30 mL) was added under ambient condition, the black solid (PtNi-NP) was precipitated and separated by centrifugation (6000 rpm, 15 min). The yellow-brown supernatant was discarded. PtNi-NP was cleaned by redispersing in a mixture of 10 mL hexane and 15 mL ethanol and separating by centrifugation for three times, and then was redispersed in hexane (20 mL) in the presence of OAc (0.05 mL) and OAm (0.03 mL). $Pt(acac)_2$ (0.25 mmol) with 100 mg 1,2-hexadecanediol and 10 mL phenyl ether were heated to 100°C for 10 min, and 20 mL hexane with PtNi-NP was slowly dropped into the synthesis system at this temperature. The synthesis system was heated to 200°C for 20 min and then cooled down to room temperature. The separation, washing, and storing proceeded at the above-mentioned conditions to obtain PtNi@Pt NPs. The hexane containing the given amount of PtNi@Pt-NP was slowly dropped into carbon black (Vulcan XC-72)/ethanol slurry to prepare the PtNi@Pt/C catalyst with a Pt loading of 20 wt %. The catalyst was heat-treated under an argon flow at 250°C for 4 h.

The particle size, size distribution, and structure of the PtNi@Pt/C catalyst were analyzed by a transmission electron microscope (TEM, JEOL2010, 200 kV). A conventional three-compartment electrochemical cell (AFCELL3, Pine) with a glassy carbon working electrode, a reversible hydrogen reference electrode (Hydroflex), and a Pt wire counter electrode was used for cyclic voltammetry (CV) and rotating disk electrode (RDE) tests of the Pt/C (20 wt % Pt, Johnson Matthey) and PtNi@Pt/C (20 wt % Pt, homemade) samples at room temperature. The ink (20 μL) with 1 mg Pt/C/ or PtNi@Pt/C per mL ethanol was dropped on the surface of glassy carbon and covered by 10 μL of 0.05 wt % Nafion. The CV tests were conducted from 0.05 to 1.1 V [vs reversible hydrogen electrode (RHE)] at a sweeping rate of 50 mV/s. The ORR polarization curves were obtained from 1.0 to 0.4 V (vs RHE) at a sweeping rate of 5 mV/s using a rotating speed of 900 rpm under oxygen (99.999%) bubbling. The working electrolyte was 0.5 M H_2SO_4.

Results and Discussion

Targeting to mimic the synthesis of the core-shell Ni(111)@Pt model nanocatalyst that possesses an ultrahigh ORR activity reported in Ref. 13, our strategy is to *i*) prepare PtNi NPs, (*ii*) coat a thin layer of Pt (≤1 nm) on the PtNi-NP to achieve Pt skin layer–Ni sublayer nanostructures, and (*iii*) deposit PtNi@Pt-NP on carbon support and heat-treat it at a mild temperature (e.g., 250°C) to remove the surfactants. The whole synthesis procedures are shown in Fig. 1. Our theoretical calculation shows that for the 4–5 nm PtNi-NP core, the thickness of the Pt shell with half moles of the Pt and Ni cores is between 0.5 and 1.0 nm, which are equal to 2–4 Pt atom layers. The electronic property of a thin Pt shell with <4 Pt atoms can be effectively modified through the sublayer Ni. For example, in Ref. 13, a single Pt atom skin layer Ni(111) sublayer was synthesized. In Ref. 7 and 8, less than 1 nm (4 atom layer) Pt surface and Fe/Co/Ni sublayer structure was prepared. Both of these nanostructured catalysts exhibit a very high ORR specific activity (SA) than the pure Pt catalyst.

Figure 2 shows the TEM images of the Pt/C and PtNi@Pt/C

* Electrochemical Society Active Member.
[z] E-mail: wzli@mtu.edu

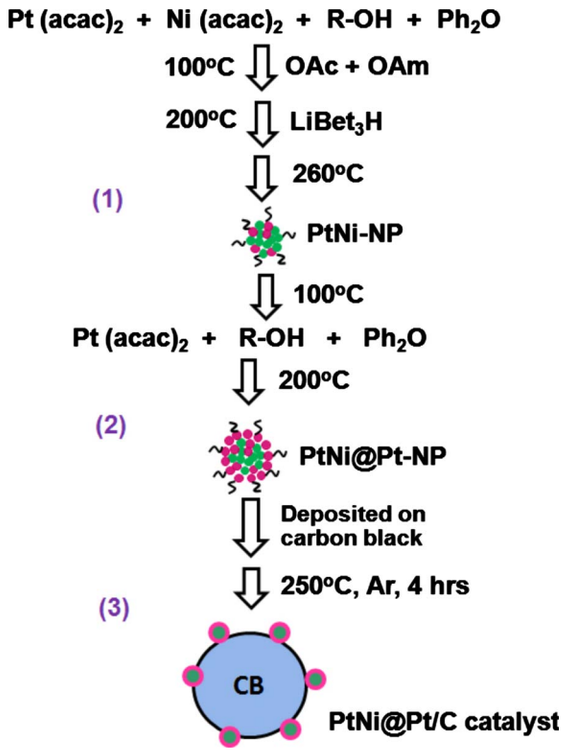

Figure 1. (Color online) Synthesis procedures of the solution-phase method for preparing carbon supported core-shell PtNi@Pt NP catalyst.

catalysts. The commercial Pt/C catalyst has small Pt NPs with a size distribution of 2–5 nm homogeneously deposited on the carbon support. The average particle size of Pt NPs is 3.4 nm. For the core-shell PtNi@Pt/C catalyst, the particle size distribution is 5–8 nm and centered at 6.2 nm. The core-shell NPs are also uniformly deposited

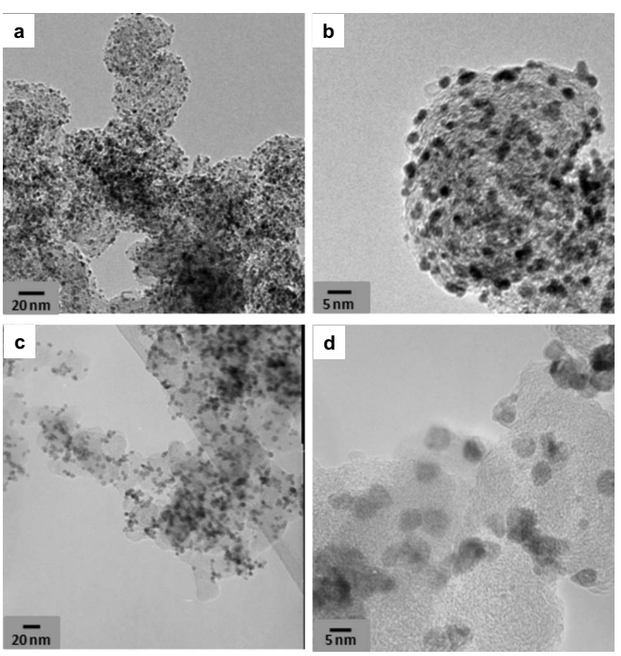

Figure 2. TEM images of Pt/C [(a) and (b)] and PtNi@Pt/C [(c) and (d)] catalysts.

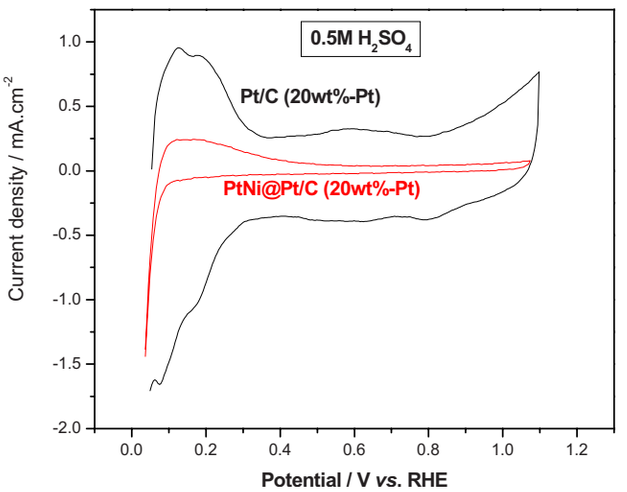

Figure 3. (Color online) Cyclic voltammograms of Pt/C and PtNi@Pt/C catalysts in 0.5 M H_2SO_4. Sweep rate: 50 mV/s, room temperature.

on the carbon surface. A few small NPs with sizes of 3–4 nm can be observed, and they are uncoated PtNi-NP and pure Pt-NP. Further work will be focused on optimizing a Pt coating process (step 2) to achieve core-shell PtNi@Pt particles with uniform compositions.

The CV curves of Pt/C and PtNi@Pt/C are shown in Fig. 3. The electrochemical surface areas (ECSAs) of Pt/C and PtNi@Pt/C are 54 and 23 m^2/g, respectively. The chemical surface areas (CSAs) of the two catalysts are 82 and 45 m^2/g. The Pt utilization can be expressed as the ratio of ECSA over CSA,[15] and they are 65.9 and 51.1% for the Pt/C and PtNi@Pt/C catalyst. The estimated surface composition of PtNi@Pt-NP is 79% Pt, which is higher than that of the commercial PtNi/C and Pt_3Ni/C (20 and 70% Pt on the surface, respectively), as reported in Ref. 12. This indicates that the PtNi@Pt/C catalyst has a Pt-rich shell; the formation can be logically attributed to the adopted two-step solution-phase reduction synthesis approach, through which more Pt can be coated on the PtNi-NP surface. In addition, surface segregation can be facilitated during the thermal treatment, leading to the Pt-rich structure.

The activity of the ORR on the two catalysts was evaluated using RDE in a three-compartment electrochemical cell, as shown in Fig. 4. The PtNi@Pt/C catalyst has a higher diffusion-limited current density i_d than Pt/C. The kinetic current density i_k can be calculated by Eq. 1, where i_o is the observed current that can be directly obtained from the ORR curve

$$i_k = (i_d \times i_o)/(i_d - i_o) \quad [1]$$

The MA of the catalyst is therefore calculated by Eq. 2

$$\text{MA} = i_k/\text{electrode mass loading} \quad [2]$$

The electrode mass loading is 20.7 $\mu g\ Pt/cm^2$. At 0.9 V (vs RHE), the MA of PtNi@Pt/C is 29.1 mA/mg Pt, which is 2.3 times higher than that of Pt/C (12.7 mA/mg Pt). The SA of the catalyst can be calculated by Eq. 3

$$\text{SA} = \text{MA/ECSA} \quad [3]$$

Because PtNi@Pt/C has a smaller ECSA than Pt/C (23 vs 54 m^2/g), the SA of PtNi@Pt/C is 5.4 times higher than Pt/C (126.5 vs 23.5 $\mu A/cm^2$). The reported ORR activity is lower than the reported data in Ref. 4 and 12. This is because (*i*) we used 0.5 M H_2SO_4, an anion-adsorption electrolyte; the current is lower than that obtained in the 0.1 M $HClO_4$ electrolyte, and (*ii*) we applied the cathodic voltage sweep (from 1.0 to 0.4 V) to collect the ORR current, which was lower than the current collected based on the anodic voltage sweep (e.g., from 0.4 to 1.0 V). Therefore, the comparison of the ORR activity on the two catalysts still holds

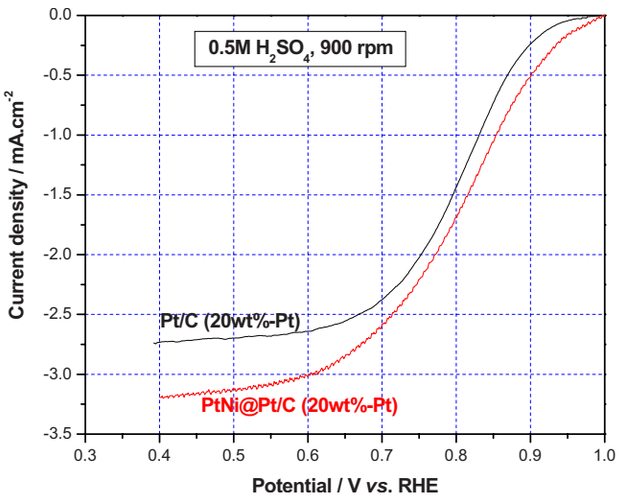

Figure 4. (Color online) Polarization curves for the ORR on Pt/C and PtNi@Pt/C catalysts by RDE in 0.5 M H_2SO_4. Sweep rate: 5 mV/s, anodic sweep, room temperature.

valid: The core-shell PtNi@Pt/C catalyst demonstrated a 5.4 times higher ORR SA than commercial Pt/C. As shown in Ref. 4, the SA of Pt–Co/C [Tanaka Kikinzoku Kogyo K.K., Japan (TKK)] is 550 μA cm_{Pt}^{-2}, which is 2.6 times higher than that of Pt/C (40 wt %, TKK) of 210 μA cm_{Pt}^{-2}. Elegant work on model catalysts has demonstrated that core-shell Ni–Pt can greatly improve the ORR SA.[7,13] Various base metal (Fe, Co, Ni, Cu, etc.) core Pt shell nanostructures have shown improved ORR activity. For example, Pt single-layer catalysts prepared by an underpotential deposition technique exhibit a high ORR activity.[16,17] Dealloyed Pt–Cu/C was reported to have an enhanced ORR activity.[18] A Pt skin layer–Ni(111) sublayer model catalyst demonstrates a 90 times higher SA than the conventional Pt/C catalyst.[13] A Pt–Fe thin-film model catalyst (<1 nm Pt skin layer and 3–4 nm Fe sublayer) demonstrates a 20 times higher ORR activity than the Pt thin film through a modified electronic structure of Pt by the sublayer base metal Fe.[7,8] The electrocatalytic ORR activity enhancement can be attributed to the modified electronic structure of the surface Pt through the underlying M (Ni, Co, and Fe) sublayer. Toda et al. proposed that the increased 5d vacancies of Pt lead to an increased 2π electron donation from O_2 to the surface Pt, resulting in an increased O_2 adsorption and weakening of the O–O bond, thus facilitating the ORR kinetics.[7,8] Stamenkovic et al., however, proposed that less anion (e.g., SO_4^{2-} and OH^-) adsorption on modified Pt electronic structure (d-band center position) is the main cause of increasing the number of active sites for O_2 adsorption and improving the ORR activity.[13]

In the current study, we introduced a wet chemical synthesis route to deliberately prepare a Ni–Pt core-shell nanostructure, which demonstrated a higher SA toward ORR than Pt/C. This synthesis strategy could potentially be extended to prepare many other core-shell structures as efficient catalysts for a wide spectrum of reactions, such as Au@Pd for formic acid oxidation and Ru@Pt for preferential oxidation of CO in hydrogen.

Conclusions

In this article, a modified solution-phase reduction method was used to prepare a PtNi@Pt/C catalyst, which has a mean particle size of 6.2 nm and uniform Pt dispersion on carbon black support. The PtNi@Pt/C catalyst demonstrated a 5.4 times higher SA than the Pt/C catalyst, which can be attributed to its modified electronic structure by the underlying Ni sublayer.

Acknowledgments

The work was partially supported by MTU start-up package D90925.

Michigan Technological University assisted in meeting the publication costs of this article.

References

1. E. Yeager, *Electrochim. Acta*, **29**, 1527 (1984).
2. T. R. Ralph and M. P. Hogarth, *Platinum Met. Rev.*, **46**, 3 (2002).
3. P. N. Ross, *Handbook of Fuel Cells: Fundamentals, Technology and Applications*, Vol. 2, p. 464, John Wiley & Sons, New York (2003).
4. H. A. Gasteiger, S. S. Kocha, B. Sompalli, and F. T. Wagner, *Appl. Catal. B*, **56**, 9 (2005).
5. V. Jalan and E. J. Taylor, *J. Electrochem. Soc.*, **130**, 2299 (1983).
6. S. Mukerjee, S. Srinivasan, M. P. Soriaga, and J. McBreen, *J. Electrochem. Soc.*, **142**, 1409 (1995).
7. T. Toda, H. Igarashi, H. Uchida, and M. Watanabe, *J. Electrochem. Soc.*, **146**, 3750 (1999).
8. T. Toda, H. Igarashi, and M. Watanabe, *J. Electroanal. Chem.*, **460**, 258 (1999).
9. V. Stamenkovic, T. J. Schmidt, P. N. Ross, and N. M. Markovic, *J. Phys. Chem. B*, **106**, 11970 (2002).
10. V. Climent, N. M. Markovic, and P. N. Ross, *J. Phys. Chem. B*, **104**, 3116 (2000).
11. N. M. Markovic, H. A. Gasteiger, and P. N. Ross, *J. Phys. Chem.*, **100**, 6715 (1996).
12. U. A. Paulus, A. Wokaun, G. G. Scherer, T. J. Schmidt, V. Stamenkovic, V. Radmilovic, N. M. Markovic, and P. N. Ross, *J. Phys. Chem. B*, **106**, 4181 (2002).
13. V. Stamenkovic, B. Fowler, B. S. Mun, G. F. Wang, P. N. Ross, C. A. Lucas, and N. M. Markovic, *Science*, **315**, 493 (2007).
14. M. T. Paffett, J. G. Beery, and S. Gottefeld, *J. Electrochem. Soc.*, **135**, 1431 (1988).
15. W. Z. Li, W. J. Zhou, Z. H. Zhou, H. Q. Li, B. Zhou, G. Q. Sun, and Q. Xin, *Electrochim. Acta*, **49**, 1045 (2004).
16. S. R. Brankovic, X. Wang, and R. R. Adzic, *Surf. Sci. Lett.*, **474**, L173 (2001).
17. Z. L. Zhang, M. B. Vukmirovic, Y. Xu, M. Mavrikakis, and R. R. Adzic, *Angew. Chem., Int. Ed.*, **44**, 2132 (2005).
18. S. Koh and P. Strasser, *J. Am. Chem. Soc.*, **129**, 12624 (2007).
19. W. Z. Li and P. Haldar, *Electrochem. Commun.*, **11**, 1195 (2009).
20. W. Z. Li, Z. W. Chen, L. B. Xu, and Y. Yan, *J. Power Sources*, **195**, 2534 (2010).
21. S. H. Sun, C. B. Murray, D. Weller, L. Folks, and A. Moser, *Science*, **287**, 1989 (2000).
22. S. H. Sun, S. Anders, T. Thomson, J. E. E. Baglin, M. F. Toney, H. F. Hamann, C. B. Murray, and B. D. Terris, *J. Phys. Chem. B*, **107**, 5419 (2003).